PHYSICAL REVIEW D **77,** 015002 (2008)

Zooming in on light relic neutralinos by direct detection and measurements of galactic antimatter

A. Bottino,[1,*] F. Donato,[1,†] N. Fornengo,[1,‡] and S. Scopel[2,§]

[1]*Dipartimento di Fisica Teorica, Università di Torino, Istituto Nazionale di Fisica Nucleare, Sezione di Torino, via P. Giuria 1, I-10125 Torino, Italy*

[2]*Korea Institute for Advanced Study, Seoul 130-722, Korea*

(Received 9 October 2007; published 8 January 2008)

The DAMA Collaboration has recently analyzed its data of the extensive WIMP direct search (DAMA/NaI) which detected an annual modulation, by taking into account the channeling effect which occurs when an ion traverses a detector with a crystalline structure. Among possible implications, this Collaboration has considered the case of a coherent weakly interacting massive particle (WIMP)-nucleus interaction and then derived the form of the annual modulation region in the plane of the WIMP-nucleon cross section versus the WIMP mass, using a specific modeling for the channeling effect. In the present paper we first show that light neutralinos fit the annual modulation region also when channeling is taken into account. To discuss the connection with indirect signals consisting in galactic antimatter, in our analysis we pick up a specific galactic model, the cored isothermal-sphere. In this scheme we determine the sets of supersymmetric models selected by the annual modulation regions and then prove that these sets are compatible with the available data on galactic antiprotons. We comment on implications when other galactic distribution functions are employed. Finally, we show that future measurements on galactic antiprotons and antideuterons will be able to shed further light on the populations of light neutralinos singled out by the annual modulation data.

DOI: 10.1103/PhysRevD.77.015002 PACS numbers: 95.35.+d, 11.30.Pb, 12.60.Jv, 95.30.Cq

I. INTRODUCTION

In a recent paper [1] the DAMA Collaboration has analyzed the data of its extensive weakly interacting massive particle (WIMP) direct search (DAMA/NaI) [2] which measured an annual modulation effect at 6.3σ C.L., by taking into account the channeling effect. This effect occurs when an ion traverses a detector with a crystalline structure [3]. In Ref. [1] implications of channeling have been discussed in terms of a specific modeling of this effect for the case of the DAMA NaI(Tl) detector; it is shown that the occurrence of channeling makes the response of this detector to WIMP-nucleus interactions more sensitive than in the case in which channeling is not included. Therefore, when applied to a WIMP with a coherent interaction with nuclei, the inclusion of the channeling effect implies that the annual modulation region, in the plane of the WIMP-nucleon cross section versus the WIMP mass, is considerably modified as compared to the one derived without including channeling. The extent of the modification depends on the specific model—dependent procedure employed in the evaluation of the channeling effect [1].

These properties are shown in Fig. 1, where the quantity $\sigma_{\rm scalar}^{\rm nucleon}$ denotes the WIMP-nucleon scalar cross section, $\xi = \rho_{\rm WIMP}/\rho_0$ is the WIMP local fractional matter density and m_χ is the WIMP mass. The dashed line denotes the annual modulation region derived by the DAMA Collaboration without including the channeling effect [2]. The solid line shows the annual modulation region derived by the same collaboration when the channeling effect is included as explained in Ref. [1].

The regions displayed in Fig. 1 are derived by varying the WIMP galactic distribution function (DF) over the set considered in Ref. [4] and by taking into account other uncertainties of different origins [1,5]. Figure 1 shows that the effect of taking channeling into account is that the annual modulation region modifies its contour with an extension towards lighter WIMP masses. Most remarkably, for WIMP masses $\lesssim 30$ GeV, the WIMP-nucleon cross section involved in the annual modulation effect decreases sizably, up to more than an order of magnitude. As mentioned before, the specific shape of the annual modulation region depends on the way in which channeling is modeled [1].

These features are of great importance for a specific dark matter candidate, the light neutralino, which was extensively investigated in Refs. [6–8]. Actually, in these papers we analyzed light neutralinos, i.e. neutralinos with a mass $m_\chi \lesssim 50$ GeV, which arise naturally in supersymmetric models where gaugino mass parameters are not related by a GUT-scale unification condition. In Refs. [6,7] it is proved that, when R-parity conservation is assumed, these neutralinos are of great relevance for the DAMA/NaI annual modulation effect. In these papers it is also shown that in the minimal supersymmetric standard model (MSSM) without gaugino mass unification the lower limit of the neutralino mass is $m_\chi \gtrsim 7$ GeV [9].

In Fig. 1, superimposed to the annual modulation regions is the scatter plot of the supersymmetric configurations of our model, whose features are summarized in the

*bottino@to.infn.it
†donato@to.infn.it
‡fornengo@to.infn.it
§scopel@kias.re.kr

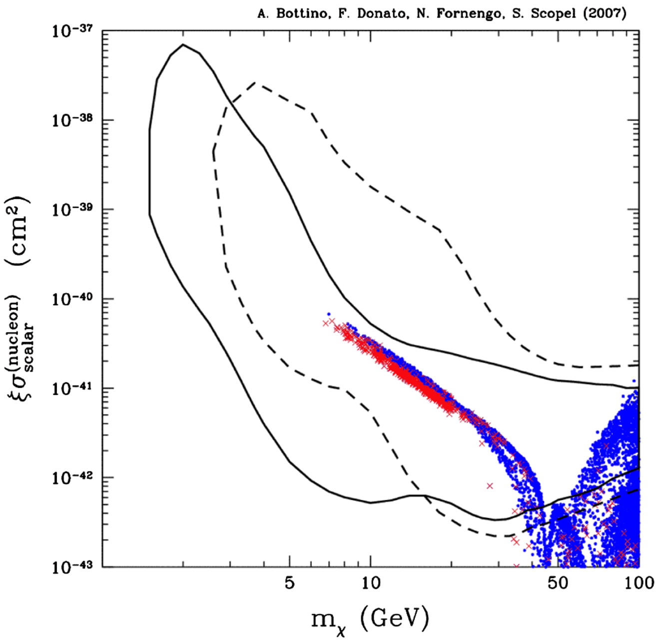

FIG. 1 (color online). WIMP-nucleon scattering cross section as a function of the WIMP mass. The solid (dashed) line denotes the annual modulation region derived by the DAMA Collaboration with (without) the inclusion of the channeling effect. The two regions contain points where the likelihood- function values differ more than 4σ from the null hypothesis (absence of modulation). These regions are obtained by varying the WIMP galactic distribution function (DF) over the set considered in Ref. [4] and by taking into account other uncertainties of different origins [1]. The scatter plot represents supersymmetric configurations calculated with the supersymmetric model summarized in the appendix. The (red) crosses denote configurations with a neutralino relic abundance which matches the WMAP cold dark matter amount ($0.092 \leq \Omega_\chi h^2 \leq 0.124$), while the (blue) dots refer to configurations where the neutralino is subdominant ($\Omega_\chi h^2 < 0.092$).

appendix. One sees that, also when the channeling effect is taken into account, the light neutralinos of our supersymmetric model fit quite well the annual modulation region.

In the present paper we consider the phenomenological consequences for light neutralinos when the annual modulation region is the one indicated by the solid line in Fig. 1. More specifically we examine the properties of our supersymmetric population of light relic neutralinos in terms of the possible antimatter components generated by their pair annihilation in the galactic halo.

To do this, we have to resort to a specific form for the WIMP DF. We take as our representative DF a standard cored isothermal-sphere model, though we do not mean to associate to this model prominent physical motivations as compared to other forms of DFs. Analyses similar to the one we present here for the cored isothermal-sphere can be developed for other galactic models. We will comment about some of them, selected among those considered in Ref. [4] (we will follow the denominations of this reference to classify our DFs).

The scheme of the present paper is the following. In Sec. II, we show how the model presented in Refs. [6–8] fits the DAMA/NaI annual modulation regions of Ref. [1] for the case of the cored isothermal-sphere model. In Sec. III we combine these results with constraints derivable from available data on cosmic antiprotons; we also discuss the sensitivity of upcoming measurements on cosmic antiprotons for investigating the neutralino populations selected by the annual modulation regions. Complementary investigations by measurements of galactic antideuterons are presented in Sec. IV. Conclusions are drawn in Sec. V. The main features of the supersymmetric scheme adopted here are summarized in the appendix.

II. THE ANNUAL MODULATION REGION IN VARIOUS HALO MODELS

As mentioned above, in the present paper we take the cored isothermal sphere as the representative model for our detailed evaluations. Similar analyses can be developed for other galactic models; we will comment about some of them. The density profile of the cored—isothermal sphere (denoted as Evans logarithmic model, or A1 model, in Ref. [4]) is:

$$\rho(r) = \frac{v_0^2}{4\pi G} \frac{3R_c^2 + r^2}{(R_c^2 + r^2)^2}, \tag{1}$$

where G is the Newton's constant, v_0 is the local value of the rotational velocity, and R_c is the core radius.

The value $R_c = 5$ kpc will be used for the core radius. For the parameter v_0 we will consider the values $v_0 = 170$, 220, 270 km sec^{-1}, which represent the minimal, central and maximal values of v_0 in its physical range [10]. For each value of v_0, we will consider the minimal and the maximal values of the local dark matter density, $\rho_0^{\min}$ and $\rho_0^{\max}$, as determined in Ref. [4]. Then, specifically, we will discuss the following sets of values: (i) $v_0 = 170$ km sec^{-1} with $\rho_0^{\min} = 0.20$ GeV cm^{-3} and $\rho_0^{\max} = 0.42$ GeV cm^{-3}; (ii) $v_0 = 220$ km sec^{-1} with $\rho_0^{\min} = 0.34$ GeV cm^{-3} and $\rho_0^{\max} = 0.71$ GeV cm^{-3}; (iii) $v_0 = 270$ km sec^{-1} with $\rho_0^{\min} = 0.62$ GeV cm^{-3} and $\rho_0^{\max} = 1.07$ GeV cm^{-3}.

Now, we turn to a comparison of the DAMA/NaI annual modulation regions of Ref. [1] with the theoretical predictions of our supersymmetric model. Figure 2 displays the DAMA annual modulation regions in the case of the A1 model [11]; the various insets correspond to the representative values of the parameters v_0 and ρ_0 previously defined. The regions of Fig. 2 are derived by the DAMA Collaboration from their data of Ref. [2], taking into account the channeling effect and under the hypothesis that the WIMP-nucleus interaction is coherent. They represent regions where the likelihood-function values differ more than 4σ from the null hypothesis (absence of modulation) [12]. The scatter plot is the same as in Fig. 1. It is remarkable that light neutralinos are able to provide a good fit to the experimental data. This occurs for values of v_0

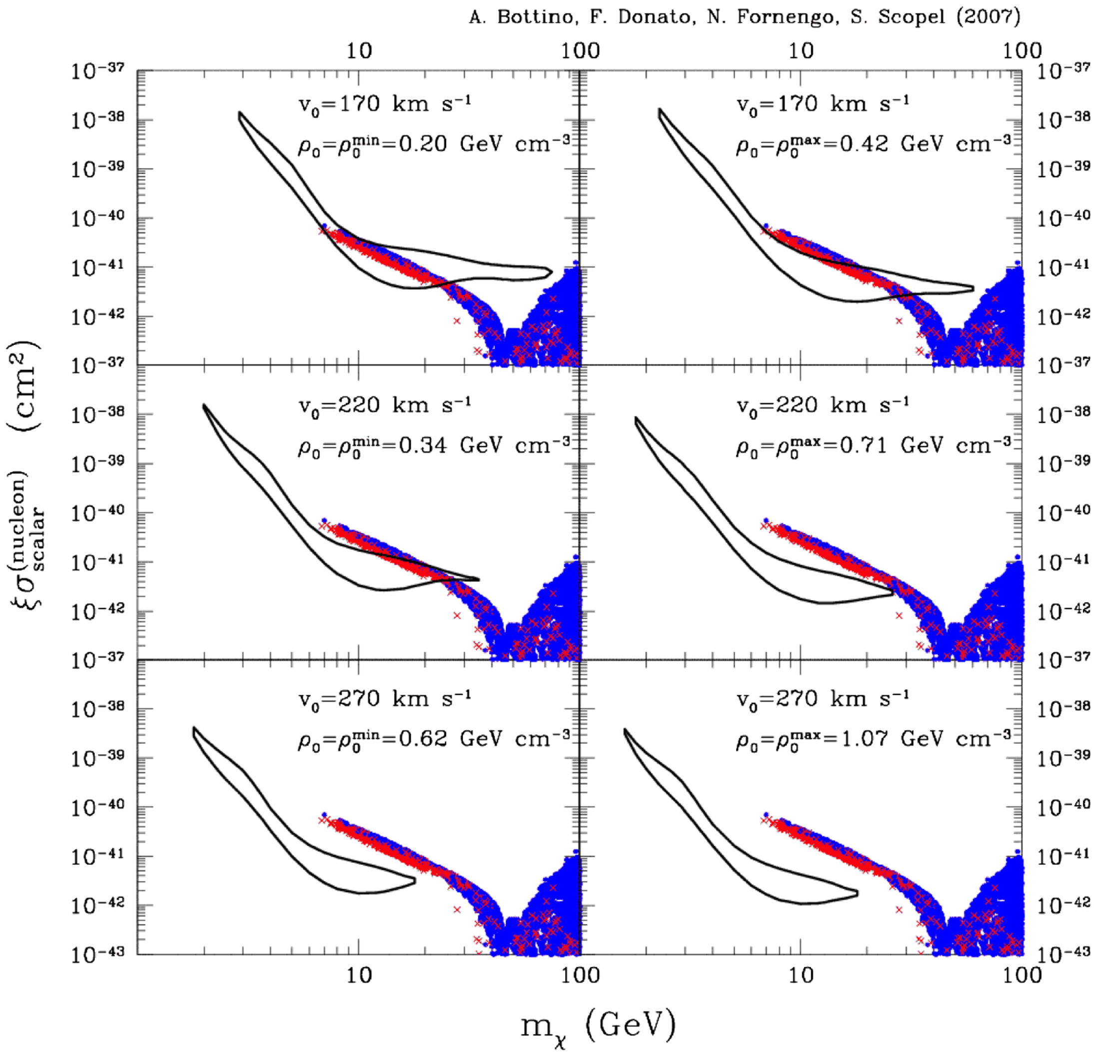

FIG. 2 (color online). WIMP-nucleon scattering cross section as a function of the WIMP mass. The solid contours denote the DAMA/NaI annual modulation regions for a cored isothermal halo, derived by including the channeling effect with the model explained in Ref. [1]. The different panels refer to different galactic halo-model parameters, according to the analysis of Ref. [4]: v_0 is the local rotational velocity, ρ_0 is the local dark matter density. The scatter plot shows the configurations for neutralino-nucleon scattering in gaugino nonuniversal supersymmetric models. The (red) crosses denote configurations with a neutralino relic abundance which matches the WMAP cold dark matter amount ($0.092 \leq \Omega_\chi h^2 \leq 0.124$), while the (blue) dots refer to configurations where the neutralino is subdominant ($\Omega_\chi h^2 < 0.092$).

and ρ_0 which are in the low-medium side of their own physical ranges, *i.e.* $v_0 \simeq (170\text{–}220)$ km sec^{-1} and $\rho_0 \simeq (0.2 - 0.4)$ GeV cm^{-3}. The light neutralinos involved in this fit stay in the mass range $m_\chi \simeq (7 - 30)$ GeV. We remark that in case the channeling is not included, the DAMA regions would be sizably displaced as compared to the ones displayed in Fig. 2, similarly to what is shown in Fig. 1. An example of the effect of including channeling in the determination of the annual modulation region, when the A1 model for the DF is taken, is explicitly displayed in Fig. 7 of Ref. [1]. As already remarked before, in connection with Fig. 1, for WIMP masses $\leq$ 30 GeV, the WIMP-nucleon cross section involved in the annual modulation effect decreases sizably, when channeling is included, up to more than an order of magnitude. This implies that, not including channeling, the fit of the experimental data with light neutralinos would require values of ρ_0 ($\rho_0 \simeq (0.6 - 1)$ GeV cm^{-3}) higher than the ones previously derived. Also v_0 would be in the high side of its physical range. These properties are of relevance for the implications which will follow.

When the channeling effect is taken into account and no rotation of the halo is considered, it turns out [12] that the features of the annual modulation region in the $m_\chi - \xi\sigma_{scalar}^{nucleon}$ plane do not differ much when the galactic DF is varied, for many of the galactic DFs considered in Ref. [4]. Thus, for instance, for a matter density with a Navarro-Frenk-White profile (A5 model of Ref. [4]) or for an isothermal model with a nonisotropic velocity dispersion (B1 model of Ref. [4]) the physical situation is very similar to the one depicted in Fig. 2. However, in the case of DFs with triaxial spatial distributions (within the class D of Ref. [4]) and for models with a corotating halo there can be an elongation of the annual modulation region towards heavier masses [1]. Further insight into the properties of light neutralinos are expected from the future results of the DAMA/LIBRA experiment [2].

We wish also to stress that the distribution of WIMPs in the Galaxy could deviate from the models mentioned above, mainly because of the presence of streams. For modification of the annual modulation region in these instances see Ref. [2]. It is worth mentioning that in the numerical derivation given above, also uncertainties of other origin may intervene. Suffice it to mention that the sizeable uncertainties which affect strength of the coupling of the neutralino to the nucleon [13].

In this paper, among the searches for WIMP direct detection we discuss only the DAMA/NaI experiment, since this is the only experiment having at present the capability to measure the annual modulation effect, which is a distinctive feature for discriminating the signal against the background in a WIMP direct search [14]. For updated reviews about other experiments of WIMP direct detection, see Ref. [15].

III. GALACTIC ANTIPROTONS

As shown in Ref. [8], among the various searches for indirect signals due to annihilation of light WIMPs, the cosmic rays antiprotons provide the most significant constraints. For this reason we now examine how this kind of limits applies to the light neutralinos singled out by the DAMA/NaI annual modulation regions.

So-called secondary antiprotons are produced in the Galaxy via interaction of proton and helium cosmic rays with the interstellar hydrogen and helium nuclei. A thorough calculation of the secondary antiproton spectrum has been performed in Ref. [16], where the antiprotons generated by spallation processes are propagated using a two-zone diffusion model described in terms of five parameters. Two of these parameters, K_0 and δ, enter the expression of the diffusion coefficient:

$$K = K_0 \beta R^{\delta}, \tag{2}$$

where R is the particle rigidity. The other three parameters are the Alfén velocity V_A, the velocity of the convective wind V_c, and the thickness L of the two large diffusion layers which sandwich the thin galactic disk. In Ref. [16] it is shown that the experimental antiproton spectrum is fitted quite well by the secondary component from cosmic-rays spallation (with a $\chi^2 = 33.6$ with 32 data points), calculated with the set of the diffusion parameters which is derived from the analysis of the boron-to-carbon ratio (B/C) component of cosmic-rays. The values of this set of best-fit parameters (denoted as median), together with their 4σ uncertainty intervals, are given in Table I. The theoretical uncertainty on the diffusion parameters reflects into a (10–20)% uncertainty on the calculated spectrum of secondary antiprotons.

TABLE I. Astrophysical parameters of the two-zone diffusion model for galactic cosmic-rays propagation, compatible with B/C analysis [16] and yielding the maximal, median and minimal primary antiproton flux.

case	δ	K_0 [kpc^2/Myr]	L [kpc]	V_c [km s^{-1}]	V_A [km s^{-1}]
max	0.46	0.0765	15	5	117.6
med	0.70	0.0112	4	12	52.9
min	0.85	0.0016	1	13.5	22.4

Primary antiproton fluxes can be generated by annihilation of neutralino pairs. We have evaluated these fluxes for the supersymmetric configurations selected by the annual modulation regions, i.e. the light neutralino populations which stay inside the annual modulation regions displayed in the insets of Fig. 2. These correspond to the cases: (A) $v_0 = 170$ km sec^{-1}, $\rho_0 = \rho_0^{\min} = 0.20$ GeV cm^{-3}; (B) $v_0 = 170$ km sec^{-1}, $\rho_0 = \rho_0^{\max} = 0.42$ GeV cm^{-3}; (C) $v_0 = 220$ km sec^{-1}, $\rho_0 = \rho_0^{\min} = 0.34$ GeV cm^{-3}.

The antiproton fluxes originated in the dark halo by the neutralino pair-annihilation processes have then been propagated in the diffusive halo using the three sets of diffusion parameters (minimal, median and maximal) given in Table I. The procedure for the evaluation of these fluxes is the one illustrated in Refs. [8,17,18]. As it was shown in Ref. [17], the uncertainty in the diffusion/propagation parameters, contrary to the case of the secondary antiprotons, induces a large uncertainty on the primary flux.

To show quantitatively how the experimental data can constrain our supersymmetric configurations, in Fig. 3 we display the (top-of-the-atmosphere) antiproton flux evaluated at a specific value of the antiproton kinetic energy, $T_{\bar{p}} = 0.23$ GeV, for the three populations A, B, and C defined above. The shaded (yellow) region denotes the amount of primary antiprotons which can be accommodated at $T_{\bar{p}} = 0.23$ GeV without entering in conflict with the BESS experimental data [19] and secondary antiprotons evaluations [16]. The dashed horizontal line denotes our estimated sensitivity of the PAMELA detector [20] to exotic antiprotons after a 3 years running: it corresponds to the admissible excess within the statistical experimental uncertainty if the measured antiproton flux consists only in the background (secondary) component. The estimate has been performed by using the background calculation of Ref. [16], and refers to a $1 - \sigma$ statistical uncertainty. All the supersymmetric configurations in Fig. 3 above the dashed line can be potentially identified by PAMELA as a signal over the secondaries, while those which are below the dashed curve will not contribute enough to the total flux

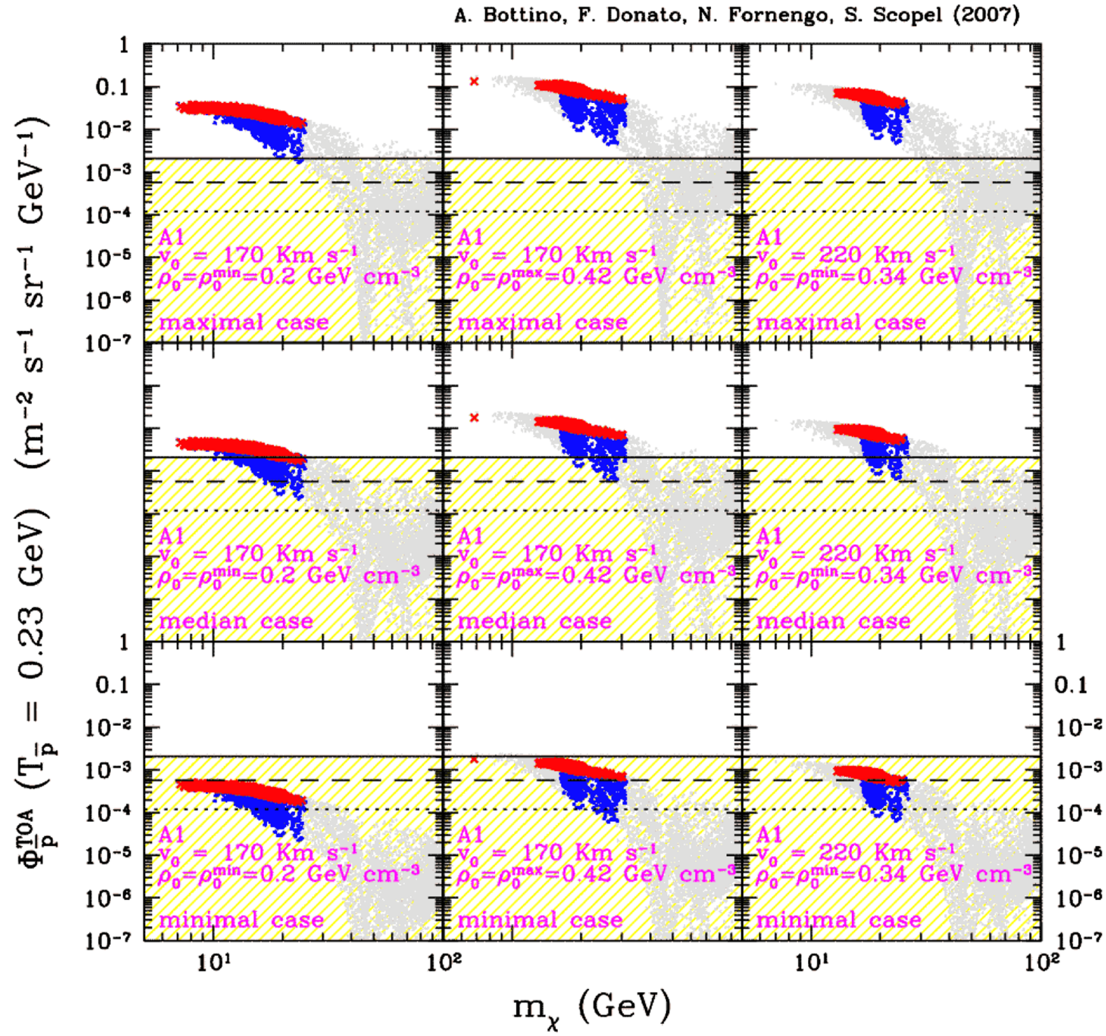

FIG. 3 (color online). Antiproton flux at $\bar{p}$ kinetic energy $T_{\bar{p}} = 0.23$ GeV, as a function of the WIMP mass and for a cored isothermal halo. Each raw corresponds to a different set of cosmic-rays propagation parameters: the upper, median and lower rows refer to the set which provides the maximal, median and minimal antiproton flux, according to the analysis of Ref. [17]. The light gray points denote configurations with a neutralino-nucleon scattering cross section outside the corresponding DAMA/NaI allowed region. The bold (colored) points refer to configurations compatible with the DAMA/NaI regions. These last points are further differentiated as follows: (red) crosses denote configurations with a neutralino relic abundance which matches the WMAP cold dark matter amount ($0.092 \leq \Omega_\chi h^2 \leq 0.124$), while (blue) dots refer to configurations where the neutralino is subdominant ($\Omega_\chi h^2 < 0.092$). The solid horizontal line shows the maximal allowable amount of antiprotons in the BESS data [19] over the secondary component; the dashed and dotted lines denote estimates of the PAMELA and AMS sensitivities to exotic antiprotons for 3 years missions, respectively.

in order to be disentangled from the background. The dotted horizontal line represents a similar estimate, but referred to the AMS detector [21] for a 3 years data-taking. Crosses (red) and dots (blue) denote neutralino configurations selected by the annual modulations regions and with $0.092 \leq \Omega_\chi h^2 \leq 0.124$ and $\Omega_\chi h^2 < 0.092$, respectively. Faint (gray) dots represent configurations which are outside of the annual modulation regions. Figure 3 shows that, for values of the diffusion parameters close to the minimal set, present antiprotons data do not set constraints. For values of the diffusion parameters around the median set, we have that: in case A, most of the neutralino configurations with $\Omega_\chi h^2 < 0.092$ and a few with $0.092 \leq \Omega_\chi h^2 \leq 0.124$ remain unconstrained; in cases B and C only subsets of neutralinos with $\Omega_\chi h^2 < 0.092$ survive. When the diffusion parameters approach the values of the maximal set, only very few SUSY configurations survive in case A. From Fig. 3 we see that the possibility of exploring our relevant neutralino configurations by future measurements of galactic antiprotons (PAMELA and AMS) is quite good. As was remarked in Sec. II, in case the channeling is not included, the fit of the experimental data of annual modulation with light neutralinos would imply values of ρ_0 higher than the those characterizing the sets A, B, and C, previously defined. This property, together with the fact that the antiproton flux depends on the square of ρ_0, might cause tension between the annual modulation data and the constraints implied by present measurements of galactic antiprotons.

In the previous analysis, we have considered the antiproton flux evaluated at a specific value of the antiproton kinetic energy, $T_{\bar{p}} = 0.23$ GeV. This analysis can be extended by examining the properties of a global fit to the full low-energy antiproton spectrum, using the same procedure which was used in Ref. [18]. We mentioned above that this spectrum is fitted quite well by the secondary component from cosmic-rays spallation [16]. As a conservative criterion for constraining our supersymmetric configurations, we can perform a χ^2 analysis on the antiproton data for the supersymmetric configurations compatible with the annual modulation study. As an illustrative application of this analysis, for the supersymmetric configurations compatible with each set A, B, and C, we calculate the antiproton flux for all the propagation parameter combinations which keep the B/C fit within a 4σ of uncertainty [22]. The primary and secondary fluxes are then required to fit the antiproton data at 99.5% C.L. ($\chi^2 < 60$). The results of this calculation are displayed in Fig. 4 for $m_\chi = 20$ GeV in the plane of the two diffusion parameters L and δ. We see that, depending on the specific isothermal-sphere parameters, we identify different regions of compatibility of the antiproton signal in terms of the astrophysical parameters which govern the diffusion of galactic cosmic rays.

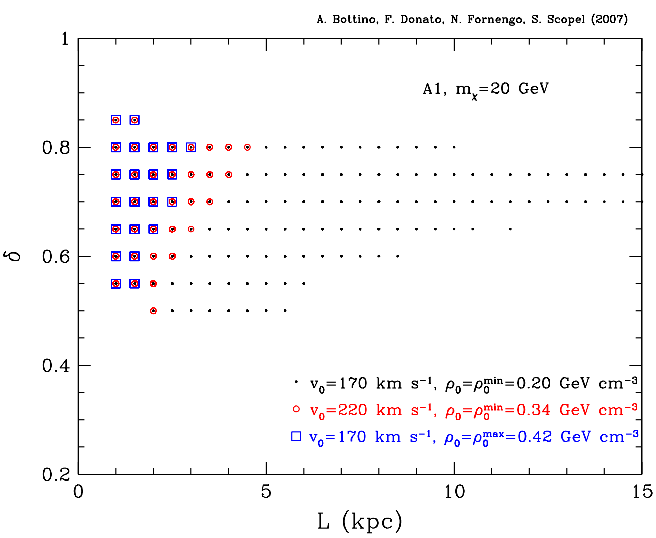

FIG. 4 (color online). Areas of compatibility between the annual modulation regions of Fig. 2 and the antiproton data for a neutralino of mass of 20 GeV, plotted in the parameter space defined by the height of the diffusive halo L and the rigidity-dependence parameter δ of the diffusion coefficient of Eq. (2). The galactic halo model is a cored-isothermal sphere. The dots, (red) squares and (blue) circles refer to: $v_0 = 170\ \mathrm{km\,sec^{-1}}$, $\rho_0 = \rho_0^{\min} = 0.20\ \mathrm{GeV\,cm^{-3}}$, $v_0 = 220\ \mathrm{km\,sec^{-1}}$, $\rho_0 = \rho_0^{\min} = 0.34\ \mathrm{GeV\,cm^{-3}}$, and $v_0 = 170\ \mathrm{km\,sec^{-1}}$, $\rho_0 = \rho_0^{\max} = 0.42\ \mathrm{GeV\,cm^{-3}}$, respectively. Each set of points shows the region in the L-δ plane which fits at 99.5% C.L. the antiproton data of BESS [19].

IV. GALACTIC ANTIDEUTERONS

Formation of antideuterons in cosmic rays proceeds through production of an antiproton and an antineutron pair by spallation (secondary production) or by WIMP pair annihilation (primary production) [23]. The coalescence process of antiproton and antineutron is easier in WIMP annihilation, since their parent particles are at rest in the galactic frame. Therefore, at low energies the primary spectrum is much enhanced as compared to the secondary one [23]. This feature makes the search for antideuterons particularly attractive for an indirect investigation of WIMPs [23,24].

The fluxes of the antideuterons produced in the dark halo by the neutralino pair-annihilation processes have been calculated following the method described in Ref. [23] and propagated in the diffusive halo using the three sets of diffusion parameters (minimal, median, and maximal) given in Table I.

In Fig. 5 we display the (top-of-the-atmosphere) antideuteron flux evaluated at the value $T_{\bar{p}} = 0.23\ \mathrm{GeV}/n$ for the three population A, B, and C defined above. The notations for the scatter plot are as in Fig. 3, that is: crosses (red) and dots (blue) denote neutralino configurations selected by the annual modulations regions and with $0.092 \leq \Omega_\chi h^2 \leq 0.124$ and $\Omega_\chi h^2 < 0.092$, respectively; faint (gray) dots represent configurations which are outside of the annual modulation regions. The horizontal dashed and dotted lines denote estimated sensitivities to antideuterons of the GAPS [25] and AMS [23] detectors.

Figure 5 shows that measurements of galactic antideuterons are perspectively very promising for investigating our light neutralino populations. Moreover, when antideuteron data will become available together with the antiproton ones, correlations in the two data sets will provide strong confidence in a possible presence of a signal, as can be appreciated by comparing Figs. 2 and 3: for most of our relevant light-mass neutralinos, a signal should be present both in the antiproton and antideuteron channel.

V. CONCLUSIONS

In the present paper we have considered the annual modulation regions which the DAMA Collaboration has recently determined, by including also the channeling effect which occurs when an ion traverses a detector with a crystalline structure, such the detector of the DAMA/NaI experiment. The inclusion of the channeling effect implies that the annual modulation region is considerably modified as compared to the one derived without including channeling. The extent of the modification depends on the specific model—dependent procedure employed in the evaluation of the channeling effect.

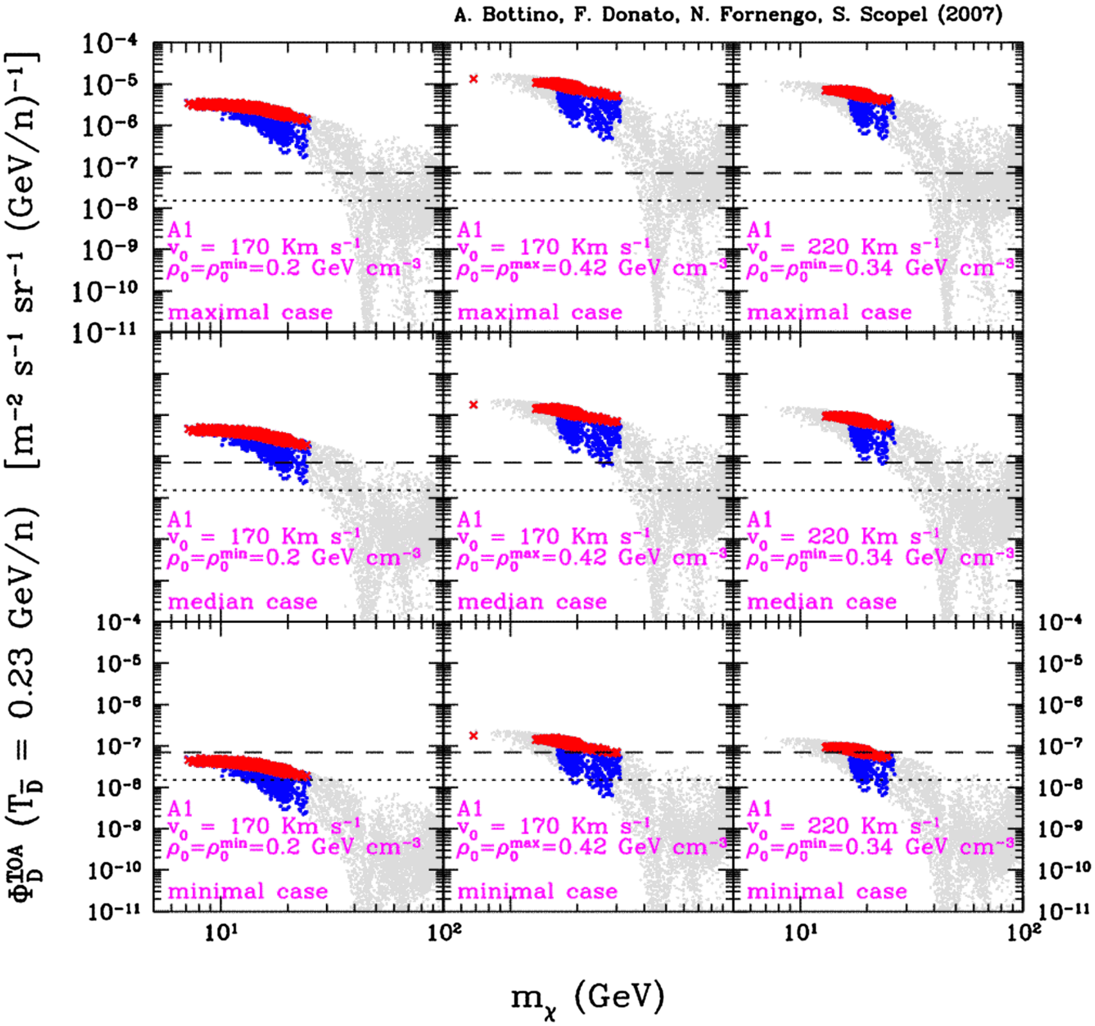

FIG. 5 (color online). Antideuteron flux at $\bar{D}$ kinetic energy $T_{\bar{D}} = 0.23$ GeV$/n$, as a function of the WIMP mass and for a cored isothermal halo. Notations are as in Fig. 3, except for the horizontal lines, which here refer to estimated sensitivities to antideuterons of the GAPS (dashed) and AMS (dotted) detectors.

In the present paper we have considered the phenomenological consequences for light neutralinos when the annual modulation region includes the channeling effect as modeled in Ref. [1]. We have proved that these annual modulation data are fitted by light neutralinos which arise naturally in supersymmetric models where gaugino mass parameters are not related by a GUT-scale unification condition.

The precise range of the neutralino mass which fits the annual modulation data depends on how the WIMP galactic distribution function is modeled and on a number of other assumptions, such as those mentioned in Sec. II. As an example, we have worked out in detail the case of a cored isothermal sphere DF. For this instance, the neutralino mass stays in the range $m_\chi \simeq$ (7–30) GeV, for values of the local rotational velocity, v_0, and of the local dark matter density, ρ_0, in the low-medium side of their own physical ranges, *i.e.* $v_0 \simeq$ (170–220) km sec^{-1} and $\rho_0 \simeq$ (0.2–0.4) GeV cm^{-3}. Similar ranges are found also in the case of a Navarro-Frenk-White profile or for an isothermal model with a nonisotropic velocity dispersion.

We have then shown that the populations of light neutralinos selected by the annual modulation regions are consistent with present data on galactic antiprotons. We have also derived the intervals of the diffusion parameters which provide this agreement in correlation with the specific galactic halo model. For instance, for neutralinos with a mass of 20 GeV and a cored isothermal model with $v_0 =$ 170 km s^{-1} we have $0.55 \lesssim \delta \lesssim 0.85$ and $L \lesssim 3$ kpc when $\rho_0 = \rho_0^{\rm max} = 0.42$ GeV cm^{-3}; instead when $\rho_0 = \rho_0^{\rm min} = 0.20$ GeV cm^{-3}, L may go up to 15 kpc with a range of δ which progressively shrinks to $\delta \sim 0.70$–0.75, when L increases.

We have also shown that future measurements of galactic antiprotons and antideuterons will offer, together with the upcoming data from DAMA/LIBRA, very interesting perspectives for further investigating the light neutralino populations selected by the annual modulation data. In case of models with a corotating halo or with triaxial spatial distributions, not investigated in the present paper, also heavier neutralinos can be involved.

Finally, a word of caution should be said concerning the fact that the distribution of WIMPs in the Galaxy could deviate from the models mentioned above, mainly because of the presence of streams and/or clumpiness. In such instances, the analysis should be appropriately adapted, along the lines discussed in the present paper.

ACKNOWLEDGMENTS

We thank the DAMA Collaboration for informing us of its work prior to publication. We are also grateful to Rita Bernabei and Pierluigi Belli for useful discussions. We acknowledge Research Grants funded jointly by Ministero dell'Istruzione, dell'Università e della Ricerca (MIUR), by Università di Torino and by Istituto Nazionale di Fisica Nucleare within the *Astroparticle Physics Project*.

APPENDIX: THE SUPERSYMMETRIC MODEL

The supersymmetric scheme we employ in the present paper is the one described in Ref. [6]: an effective MSSM scheme (effMSSM) at the electroweak scale, with the following independent parameters: M_2, μ, $\tan\beta$, m_A, $m_{\tilde{q}}$, $m_{\tilde{l}}$, A and $R \equiv M_1/M_2$. Notations are as follows: μ is the Higgs mixing mass parameter, $\tan\beta$ the ratio of the two Higgs v.e.v.'s, m_A the mass of the CP-odd neutral Higgs boson, $m_{\tilde{q}}$ is a squark soft-mass common to all squarks, $m_{\tilde{l}}$ is a slepton soft-mass common to all sleptons, A is a common dimensionless trilinear parameter for the third family, $A_{\tilde{b}} = A_{\tilde{t}} \equiv A m_{\tilde{q}}$ and $A_{\tilde{\tau}} \equiv A m_{\tilde{l}}$ (the trilinear parameters for the other families being set equal to zero).

Since we are here interested in light neutralinos, we consider values of R lower than its GUT value: $R_{\rm GUT} \simeq 0.5$. For definiteness, we take R in the range: 0.005–0.5.

In the present paper the numerical analyses are performed by a scanning of the supersymmetric parameter space, with the following ranges of the MSSM parameters: $30 \leq \tan\beta \leq 50$, $100\ \text{GeV} \leq |\mu| \leq 300\ \text{GeV}$, $100\ \text{GeV} \leq M_2 \leq 1000\ \text{GeV}$, $100\ \text{GeV} \leq m_{\tilde{q}}$, $m_{\tilde{l}} \leq 1000\ \text{GeV}$, $90\ \text{GeV} \leq m_A \leq 150\ \text{GeV}$, $-3 \leq A \leq 3$.

The following experimental constraints are imposed: accelerators data on supersymmetric and Higgs boson searches (CERN e^+e^- collider LEP2 [26] and Collider Detectors D0 and CDF at Fermilab [27]); measurements of the $b \to s + \gamma$ decay process [28]: $2.89 \leq \text{BR}(b \to s + \gamma) \times 10^4 \leq 4.21$ is employed here: this interval is larger by 25% with respect to the experimental determination [28] in order to take into account theoretical uncertainties in the SUSY contributions [29] to the branching ratio of the process (for the standard model calculation, we employ the recent NNLO results from Ref. [30]); the upper bound on the branching ratio $\text{BR}(B_s^0 \to \mu^- + \mu^+)$ [31]: we take $\text{BR}(B_s^0 \to \mu^- + \mu^+) < 1.2 \times 10^{-7}$; measurements of the muon anomalous magnetic moment $a_\mu \equiv (g_\mu - 2)/2$: for the deviation Δa_μ of the experimental world average from the theoretical evaluation within the standard model we use here the range $-98 \leq \Delta a_\mu \cdot 10^{11} \leq 565$, derived from the latest experimental [32] and theoretical [33] data.

[1] R. Bernabei *et al.* (DAMA Collaboration), arXiv:0710.0288.

[2] R. Bernabei *et al.* (DAMA Collaboration), Riv. Nuovo Cimento Soc. Ital. Fis. **26N1**, 1 (2003); Int. J. Mod. Phys. D **13**, 2127 (2004); Int. J. Mod. Phys. A **21**, 1445 (2006); Eur. Phys. J. C **47**, 263 (2006); Int. J. Mod. Phys. A **22**, 3155 (2007).

[3] J. Lindhard, Phys. Lett. **12**, 126 (1964); R. S. Nelson and N. W. Thompson, Philos. Mag. **8**, 1677 (1963); C. J. Andrean and R. L. Hines, Phys. Rev. **159**, 285 (1967); S. M. Hogg *et al.*, Appl. Phys. Lett. **80**, 4363 (2002); M. M. Bredov and N. M. Okuneva, Doklady Akad. Nauk SSSR **113**, 795 (1957); E. M. Drobyshevski, arXiv:0706.3095.

[4] P. Belli, R. Cerulli, N. Fornengo, and S. Scopel, Phys. Rev. D **66**, 043503 (2002).

[5] In deriving the regions of Fig. 1, cases A, B, C defined in Sec. 7.2 of the first paper of Ref. [2] have been included.

[6] A. Bottino, N. Fornengo, and S. Scopel, Phys. Rev. D **67**, 063519 (2003); A. Bottino, F. Donato, N. Fornengo, and S. Scopel, Phys. Rev. D **68**, 043506 (2003).

[7] A. Bottino, F. Donato, N. Fornengo, and S. Scopel, Phys. Rev. D **69**, 037302 (2004).

[8] A. Bottino, F. Donato, N. Fornengo, and S. Scopel, Phys. Rev. D **70**, 015005 (2004).

[9] For other recent determinations of a lower bound on the neutralino mass in MSSM without gaugino mass unification, see: D. Hooper and T. Plehn, Phys. Lett. B **562**, 18 (2003); G. Belanger, F. Boudjema, A. Pukhov, and S. Rosier-Lees, arXiv:hep-ph/0212227; In these papers a lower limit of ~(12–18) GeV is derived. Since only a scenario with a large mass for the CP-odd neutral Higgs boson is considered in these papers, the derived lower bound is larger than the one of Refs. [6,7].

[10] C. S. Kochanek, Astrophys. J. **457**, 228 (1996).

[11] In deriving the regions of Fig. 2, only case A defined in Sec. 7.2 of the first paper of Ref. [2] has been included.

[12] We thank the DAMA Collaboration for providing us with

the results of their analysis also for cases not displayed in Ref. [1].

[13] A. Bottino, F. Donato, N. Fornengo, and S. Scopel, Astropart. Phys. **13**, 215 (2000); Astropart. Phys. **18**, 205 (2002).

[14] A. K. Drukier, K. Freese, and D. N. Spergel, Phys. Rev. D **33**, 3495 (1986); K. Freese, J. A. Frieman, and A. Gould, Phys. Rev. D **37**, 3388 (1988).

[15] P. Belli, G. Gerbier, and D. Bauer at the "Tenth International Conference on Topics in Astroparticle and Underground Physics" (TAUP 2007), Sendai, Japan, 2007 (http://www.awa.tohoku.ac.jp/taup2007/slides/).

[16] F. Donato *et al.*, Astrophys. J. **563**, 172 (2001).

[17] F. Donato, N. Fornengo, D. Maurin, P. Salati, and R. Taillet, Phys. Rev. D **69**, 063501 (2004).

[18] A. Bottino, F. Donato, N. Fornengo, and P. Salati, Phys. Rev. D **72**, 083518 (2005).

[19] T. Maeno *et al.* (BESS Collaboration), Astropart. Phys. **16**, 121 (2001).

[20] M. Boezio *et al.*, Nucl. Phys. B, Proc. Suppl. **134**, 39 (2004); P. Picozza and A. Morselli, arXiv:astro-ph/0604207.

[21] S. Ahlen *et al.*, Nucl. Instrum. Methods Phys. Res., Sect. A **350**, 351 (1994).

[22] D. Maurin, F. Donato, R. Taillet, and P. Salati, Astrophys. J. **555**, 585 (2001).

[23] F. Donato, N. Fornengo, and P. Salati, Phys. Rev. D **62**, 043003 (2000).

[24] H. Baer and S. Profumo, J. Cosmol. Astropart. Phys. 12 (2005) 008.

[25] C. J. Hailey *et al.*, J. Cosmol. Astropart. Phys. 01 (2006) 007; J. Koglin, "The Hunt for Dark Matter", Fermilab, 2007.

[26] A. Colaleo (ALEPH Collaboration), SUSY'01, 2001, Dubna, Russia; J. Abdallah *et al.* (DELPHI Collaboration), DELPHI Report No. 2001-085 CONF 513, 2001; LEP Higgs Working Group for Higgs boson searches, arXiv:hep-ex/0107029; LEP2 Joint SUSY Working Group, http://lepsusy.web.cern.ch/lepsusy/.

[27] A. A. Affolder *et al.* (CDF Collaboration), Phys. Rev. Lett. **86**, 4472 (2001); V. M. Abazov *et al.* (D0 Collaboration), Phys. Rev. Lett. **97**, 171806 (2006).

[28] E. Barberio *et al.* (HFAG), arXiv:hep-ex/0603003.

[29] M. Ciuchini, G. Degrassi, P. Gambino, and G. F. Giudice, Nucl. Phys. **B534**, 3 (1998).

[30] M. Misiak *et al.*, Phys. Rev. Lett. **98**, 022002 (2007).

[31] V. M. Abazov *et al.* (D0 Collaboration), Phys. Rev. D **76**, 092001 (2007).

[32] G. W. Bennet *et al.* (Muon $g-2$ Collaboration), Phys. Rev. D **73**, 072003 (2006).

[33] J. Bijnens and J. Prades, Mod. Phys. Lett. A **22**, 767 (2007).